Microbial Pathogenesis 53 (2012) 87–94

Contents lists available at SciVerse ScienceDirect

Microbial Pathogenesis

journal homepage: www.elsevier.com/locate/micpath

Intraperitoneal administration of Shiga toxin 2 induced neuronal alterations and reduced the expression levels of aquaporin 1 and aquaporin 4 in rat brain

María Soledad Lucero [1], Federico Mirarchi [1], Jorge Goldstein [1], Claudia Silberstein*

Departamento de Fisiología, Facultad de Medicina, Universidad de Buenos Aires, Paraguay 2155, Buenos Aires (p.c.1121), Argentina

ARTICLE INFO

Article history:
Received 23 February 2012
Received in revised form
3 May 2012
Accepted 10 May 2012
Available online 17 May 2012

Keywords:
Hemolytic uremic syndrome
Shiga toxin 2
Water channel

ABSTRACT

Shiga toxin-producing *Escherichia coli* produces watery and hemorrhagic diarrhea, and hemolytic uremic syndrome (HUS) characterized by thrombocytopenia, microangiopathic hemolytic anemia, and acute renal failure. Central nervous system (CNS) complications are observed in around 30% of infant population with HUS. Common signs of severe CNS involvement leading to death include seizures, alteration of consciousness, hemiparesis, visual disturbances, and brain stem symptoms. The purpose of the present work was to study the effects of Shiga toxin 2 (Stx2) in the brain of rats intraperitoneally (i.p.) injected with a supernatant from recombinant *E. coli* expressing Stx2 (sStx2). Neurological alterations such as postural and motor abnormalities including lethargy, abnormal walking, and paralysis of hind legs, were observed in this experimental model of HUS in rats. Neuronal damage, as well as significant decrease in aquaporin 1 (AQP1) and aquaporin 4 (AQP4) expression levels were observed in the brain of rats, 2 days after sStx2 injection, compared to controls. Downregulation of aquaporin protein levels, and neuronal alterations, observed in brain of rats injected with sStx2, may be involved in edema formation and in neurological manifestations characteristic of HUS.

1. Introduction

Post-diarrhea hemolytic uremic syndrome (HUS) is the most common cause of acute renal failure in children in Argentina and the second leading cause of chronic renal failure in children under 5 years [1,2]. Central nervous system (CNS) complications are observed in around 30% of infant population with HUS. Moreover, about 5% of patients with HUS die during the acute phase and most of these deaths are due to the CNS damage [3–5]. Patients may suffer acute seizures, alteration of consciousness, visual disturbances, irritability, hemiparesis, and motor disorders [3,6–8].

Clinical and histological renal and CNS damages have been strongly associated with Shiga toxin type 1 and/or 2 (Stx1, Stx2) produced by *Escherichia coli* O157:H7 and other related bacterial strains frequently isolated from children with HUS, although strains expressing Stx2 are highly prevalent in Argentina [9]. Stx contains an A subunit monomer (32 kDa) bound non-covalently to five B subunits (7.7 kDa) [10]. The B subunit pentamer binds to the glycolipid globotriaosylceramide (Gb3) on the plasma membrane of target cells [11], followed by the holotoxin internalization into the cell and transport to the endoplasmic reticulum by a retrograde pathway [12]. Then, the A subunit exhibits RNA N-glycohydrolase activity and cleaves a specific adenine residue on the 28S ribosomal RNA in the cytosol, thereby inhibiting protein synthesis [13,14].

The brain expresses Gb3, which may account, at least in part, for brain-targeting of Stx in HUS. The Gb3 was described to be localized in neurons and endothelial cells of the human CNS and in neurons of normal and Stx2 exposed mice [15]. Intracerebroventricular administration of Stx2 in rat brains increased the expression of Gb3 in neurons from striatum, hippocampus and cortex [16], and induced striatal neuronal death as well as glial alteration with perivascular astrocyte cytoplasmic edema and astrocyte gliofilament hypertrophy [17].

Piglets inoculated with *E. coli* O157:H7 that produced Stx2 developed neurological symptoms including convulsions, vascular damage with pyknosis and karyorrhexis of brain endothelial cells as well as brain edema [18,19]. Moreover, mice inoculated intragastrically with *E. coli* O157:H7 developed flaccid paralysis associated with brain edema and microhemorrhage [20].

Abbreviations: AQP, aquaporin; CNS, central nervous system; Gb3, globotriaosylceramide; GFAP, glial fibrillary acid protein; HUS, hemolytic uremic syndrome; IOD, integral optical density; IL-1β, interleukin-1beta; i.p., intraperitoneally; LPS, lipopolysaccharide; PBS, phosphate-buffered saline; sCtrl, control supernatant; sStx2, supernatant from recombinant *E. coli* expressing Stx2; Stx, Shiga toxin; Stx2, shiga toxin 2; TNF-α, tumor necrosis factor-alpha.

* Corresponding author. Tel.: +54 11 5950 9500x2133.
E-mail addresses: csilber@fmed.uba.ar, silberstein.claudia@gmail.com (C. Silberstein).
[1] Tel.: +54 11 5950 9500x2133.

0882-4010/$ – see front matter © 2012 Elsevier Ltd. All rights reserved.
doi:10.1016/j.micpath.2012.05.005

The presence of edema and neurological manifestations as convulsions have been related to alteration in the expression levels of aquaporins (AQPs) in brain, found in different CNS diseases [21–23]. However, no reports have been published before about AQPs observations in CNS of animal models or patients with HUS.

The water channels AQP1 and AQP4 are abundantly expressed in the mammalian brain, being major contributors for brain fluid volume homeostasis. The AQP1 is strongly expressed in the apical membrane of the choroid plexus epithelium lining the ventricles [24] and is implicated in the cerebrospinal fluid production. The AQP4 is expressed in the foot processes of astrocytes in direct contact with capillaries, and in the glia limitants of rats and human brain [25]. The AQP4 is also expressed in the basolateral membrane of the ependymal cells lining the ventricles [25]. Two distinct isoforms (M1 and M23) of AQP4 have been identified with different translation initiation sites [26]. The M23-AQP4 forms characteristic orthogonal arrays of intramembraneous particles while the M1-AQP4 does not form orthogonal arrays [27,28]. These proteins are implicated in brain edema formation and they are believed to participate in potassium clearance during neuronal activation [29,30].

Recently, we have developed an experimental model of HUS in weaned Sprague–Dawley rats [31]. Rats, intraperitoneally (i.p.) injected with a supernatant from recombinant *E. coli* expressing Stx2 (sStx2), developed acute renal failure, intestinal alterations, and died 3–5 days after Stx2 injection [31]. In the present work, we have analyzed the histopathological damage as well as the expression levels of AQP1 and AQP4 proteins in the brain of a rat experimental model of HUS.

2. Materials and methods

2.1. Stx2 supernatant

The Stx2 supernatant was produced as previously described [31]. Briefly, Stx2 gene was cloned into pGEM-T-Easy, and recombinant *E coli* DH5α expressing Stx2 were cultured overnight at 37 °C in Luria-Bertani broth supplemented with 100 μg/ml ampicillin (Sigma–Aldrich, St. Louis, MO, USA). Bacterial cells were then removed by centrifugation, and the supernatant from recombinant *E. coli* expressing Stx2 (sStx2) was filtered through 0.22 μm pore size filter units (Millipore Corp., Billerica, MA, USA). A control supernatant (sCtrl) was prepared from a recombinant *E coli* that contained only the plasmid.

Cytotoxic activity of sStx2 was measured by neutral red uptake in Vero cells, and lipopolysaccharide (LPS) content was determined using the HEK-Blue LPS Detection Kit (InvivoGen, San Diego, USA). Both sStx2 and sCtrl supernatants contained the same concentration of LPS (30 ng LPS/ml). Immunoblot analysis using the monoclonal antibodies against the A and B subunits (Biodesign International, ME, USA) of Stx2 showed that sStx2 expressed StxA and StxB [17].

2.2. Experimental model of HUS in rats

Male Sprague–Dawley rats were obtained from the animal facility at the School of Veterinarian, Universidad de Buenos Aires. The rats were individually housed under controlled conditions of illumination, humidity, and temperature, with food and water being available *ad libitum*. Animals were allowed 3–7 days to adapt to housing conditions before undergoing any manipulation. Animal studies were conducted using protocols approved by the Institutional Animal Care and Use Committee and Scientific Program of the Universidad de Buenos Aires.

The development of the model of HUS in rats has been previously described [17]. Weaned male Sprague–Dawley rats (70–100 g, 4 weeks old) were i.p. injected with 1 ml/100 g body weight (b.w.) of sStx2 (400 ng Stx2/ml). Control rats were i.p. injected with 1 ml/100 g b.w. of sCtrl. Two days after sStx2 injection rats were i.p. anesthetized (100 μg ketamine and 10 μg diazepam/g b.w.) and sacrificed. For western blot studies, brains were removed and quickly frozen. For morphological and immunofluorescence studies, rats were perfused with 10% formol or 4% paraformaldehyde in phosphate-buffered saline (PBS) 0.1 M (pH 7.4) followed by the removal of the brain.

2.3. Histopathology analysis

The brain was quickly extracted and fixed in 10% formol in 0.1 M PBS (pH 7.4). The tissue sections were dehydrated and embedded in paraffin. Sections of 5 μm were made with a microtome (Leica RM 2125, Wetzlar, Germany) and mounted on 2% silane-coated slides. Sections were stained with Nissl, and observed by light microscopy (Nikon Eclipse 200, NY, USA).

2.4. Immunofluorescent detection of AQP1, AQP4, and GFAP

Brain sections were blocked with 5% fetal bovine serum in PBS for 1 h, following incubation with affinity-purified polyclonal rabbit IgG anti-AQP1 (Alpha Diagnostic, San Antonio, USA), or rabbit IgG anti-AQP4 (Santa Cruz, CA, USA) antibodies, dilution 1:100 in PBS for 16 h at 4 °C. After several rinses with the same buffer, sections were incubated 1 h with Cy3-conjugated goat Anti-rabbit (Jackson ImmunoResearch Lab., PA, USA) secondary antibody, dilution 1:400.

Double fluorescence staining was performed for AQP4 and GFAP. For this purpose, brains were removed from the skull, and post-fixed in 4% paraformaldehyde in PBS 0.1 M, pH 7.4. Frozen slices were washed, permeabilised with Triton X-100 (0.25%v/v)(TX-100), and blocked (5% bovine serum albumin in PBS) for 2 h. After incubation with Anti-AQP4 antibodies, as explained above, slices were then incubated for 2 h with IgG chicken Anti-GFAP, (1:200 dilution in PBS, with 2% BSA, and 0.25% TX-100; Neuromics, Edina, MN). After washing, slices were incubated with an FITC-conjugated Anti-Chicken, IgG antibody (1:400 dilution in PBS, with 2% BSA, and 0.25% v/v TX-100; Jackson ImmunoResearch Lab., PA, USA) for 1 h at room temperature.

Negative control tests for AQP1, AQP4, and GFAP, were carried out with pre-immune serum instead of the primary antibodies. Sections were observed by light microscopy (Nikon Eclipse 2000, NY, USA) and micrographs were obtained using a digital camera. For quantification of AQP1 and AQP4 immunofluorescence, the integral optical density (IOD) was analyzed with Image J-NIH software. For statistical analysis of quantitative measurements Student's *t*-test was used.

2.5. Western blot analysis

Brains were homogenized in iced-cold lysis buffer (Tris–EDTA pH = 7,5, 150 mM NaCl, 1% Triton X-100) supplemented with protease inhibitor cocktail (Invitrogen Life Technologies, CA, USA) followed by centrifugation at 6000 rpm for 10 min at 4 °C. The supernatant was collected and stored at −80 °C. Protein content was determined using a BCA Protein Assay Kit (Pierce, Thermo Scientific, Rockford, IL, USA). Samples were diluted in Laemmli Buffer (Sigma–Aldrich) and proteins were resolved in a 10% SDS-PAGE. Samples used for AQP1 analysis were heated at 95° for 5 min, while samples used for AQP4 analysis were not heated before being loaded in the gel. Following electrophoresis,

immunoblotting was performed by electrotransferring the proteins to a PVDF membrane (Bio-Rad laboratories, Hercules, CA, USA) in transfer buffer (25 mM Tris, 192 mM glycine, 20% methanol (v/v), pH 8.3 for AQP1; and 3 mM Na_2CO_3, 10 mM $NaHCO_3$, 0.01% SDS for AQP4). The membrane with blotted proteins was blocked for 1 h at room temperature with PBS containing 5% (w/v) skim milk powder and 0.05% Tween 20, followed by incubation, overnight at 4 °C, with polyclonal rabbit AQP1 or AQP4 (Alpha Diagnostic Intl. Inc) diluted 1:1000 and 1:500 respectively in PBS. After several washes with PBS containing 0.05% Tween 20, the membrane was incubated with a goat anti-rabbit IgG HRP-conjugated antibody (Sigma–Aldrich, St Louis, MO, USA). Peroxidase activity was visualized using chemiluminescence reagents and processed on autoradiographic film. Blots were reprobed with β-actin antibody (1:2000; mouse monoclonal antibody; Sigma–Aldrich, St Louis, MO, USA) to verify equal protein loading. Semicuantitatification of protein expression levels were analyzed with GelPro software.

3. Results

3.1. Symptoms of disease and histological observations in rats i.p. injected with sStx2

Weaned male Sprague–Dawley rats i.p. injected with sStx2 showed neurological alterations such as postural and motor abnormalities including lethargy, abnormal walking, and paralysis of hind legs, since 2 days after toxin inoculation. As it was reported previously [31], this group of animals became oliguric and significantly increased creatinine and urea serum levels, demonstrating the HUS development.

Asymmetric neurons with pyknotic and amorphous nuclei, and hypertrophied axons were found in the periventricular region of Nissl stained brain sections (Fig. 1B). Hypertrophied pyramidal neurons with pyknotic nuclei, and edema surrounding the cell bodies and the perivascular area were observed in the fourth layer of the cerebral cortex (Fig. 1D). Fig. 1F shows tissue destruction and loss of epithelial-endothelial organization in the area of the choroid plexus, that may suggest the presence of edema. Neurons, astroglia, and choroid plexus of control rats remained preserved (Fig. 1A, C, and E).

Purkinje cells in the cerebellum of rats injected with sStx2 (Fig. 1H) showed necrosis, pyknotic and asymmetric nuclei (inferior inlet Fig. 1H), and hypertrophied axons (superior inlet, Fig. 1H). Those alterations were not observed in cerebellum sections of control animals (Fig. 1G).

3.2. Expression levels of AQP1 and AQP4

Expression levels of AQP1 and AQP4 were analyzed by immunofluorescence and western blot in the brain of rats i.p. injected with sStx2 or sCtrl. As shown in Fig. 2A, AQP1 was highly expressed in the apical membrane of epithelial cells in the choroid plexus. A lesser positive staining of AQP1 was also shown in the vascular endothelium of choroid plexus (Fig. 2A). A significant decrease in AQP1 expression levels was observed in choroid plexus from rats injected with sStx2 (Fig. 2B), compared with the expression observed in brains of control rats. The decrease in AQP1 staining, calculated by the Integral optical density (IOD) (Fig. 2D), was corroborated by western blot of total brain samples (Fig. 2E). Densitometric analysis of AQP1 (Fig. 2F), normalized to beta-actin, revealed a fourfold inhibition in the aquaporin expression in brains of sStx2 injected rats compared to those of sCtrl injected rats.

In control rats, a highly positive immunoreactivity for AQP4 was found in astrocytic endfeet around blood vessels as well as in adjacent endothelial cell membranes of the cerebrum (Figs. 3A, C and 4), and the cerebellum (Fig. 3E). A bright staining for AQP4 was observed in the subarachnoid space (Fig. 3A), and in the epithelium of the ependymal cells surrounding the ventricles (Fig. 3C). A significant inhibition, of about fourfold, in the expression levels of AQP4 (Fig. 3G) was measured in the brain of rats 2 days after sStx2 inoculation (Fig. 3B, D, F). Western blot analysis, normalized to beta-actin, confirmed the immunofluorescence results (Fig. 3I) and showed a decrease of both AQP4-M1 and AQP4-M23 isoforms in total brain samples of sStx2 injected rats, compared to controls (Fig. 3H). The reduction of AQPs in the CNS produced in rats with HUS could be involved in alteration of water balance and neurological disorders.

3.3. Double fluorescence staining of AQP4 and glial fibrillary acid protein (GFAP)

We assayed whether downregulation of AQP4, found in astrocytes of rat brains 2 days after i.p. sStx2 inoculation, correlated with changes in astrocytic GFAP reactivity. Double immunofluorescence for AQP4 and GFAP showed colocalization in both sCtrl and sStx2 injected rats, in which merging yellow staining was observed in the astrocytes endfeet surrounding the vessels (Fig. 4A). In sStx2 injected rats, a significantly higher immunoreactivity for GFAP, calculated by the IOD (Fig. 4B), was found in the body of astrocytes localized in periventricular regions (Fig. 4A), compared with GFAP immunostaining of control rat brains.

4. Discussion

CNS alterations with brain damage involvement are the most common cause of death in patients with HUS [3]. In the present work, histopathological alterations are shown in brain of weaned male Sprague–Dawley rats i.p. injected with a filtered supernatant from recombinant *E. coli* expressing Stx2. Since 2 days after Stx2 injection, neuronal damage was observed in brain periventricular and cortical regions, and in cerebellar Purkinje cells, which correlates with the neurological manifestations observed in this group of animals. Moreover, the expression analysis of AQP1 and AQP4, the main water channels present in CNS, showed a significant decrease of these proteins in brain of sStx2 injected rats, compared with sCtrl injected animals.

The neurological manifestations, such as postural and motor abnormalities, and lethargy, observed in sStx2 injected rats, may be explained by the damage of pyramidal neurons of cerebral cortex. Upper motor neurons project their pathways from the cerebral cortex to the lower end of the spinal cord. Damage to these neurons or their descending motor pathways produces severe hypotonia, particularly in the limbs, as the activity of spinal circuits is suddenly deprived of motor cortex and brain stem afferents [32]. Moreover, the damage of Purkinje neurons, observed in sStx2 inoculated rats, can also be associated with alterations in cerebellum-dependent motor behaviors. The cerebellum is involved in motor and balance coordination as well as learning and memory processes, in which Purkinje cells serve as the only output neurons of the cerebellar cortex. Neurons with pyknotic and amorphous nuclei, and hypertrophied axons were found in the group of rats inoculated with the toxin. These observations are consistent with those obtained in previous studies, in which hypertrophic and demyelinated axons, and neuronal apoptosis, were observed in rats intracerebroventricularly inoculated with Stx2 [17]. Other studies performed in mice i.p. injected with Stx2 demonstrated that neurons are targets of Stx2 through Gb3 receptor, affecting neuronal function which leads to paralysis [15].

AQP4 expression in astrocytic foot processes in direct contact with blood vessels, suggests AQP4 involvement in water transport

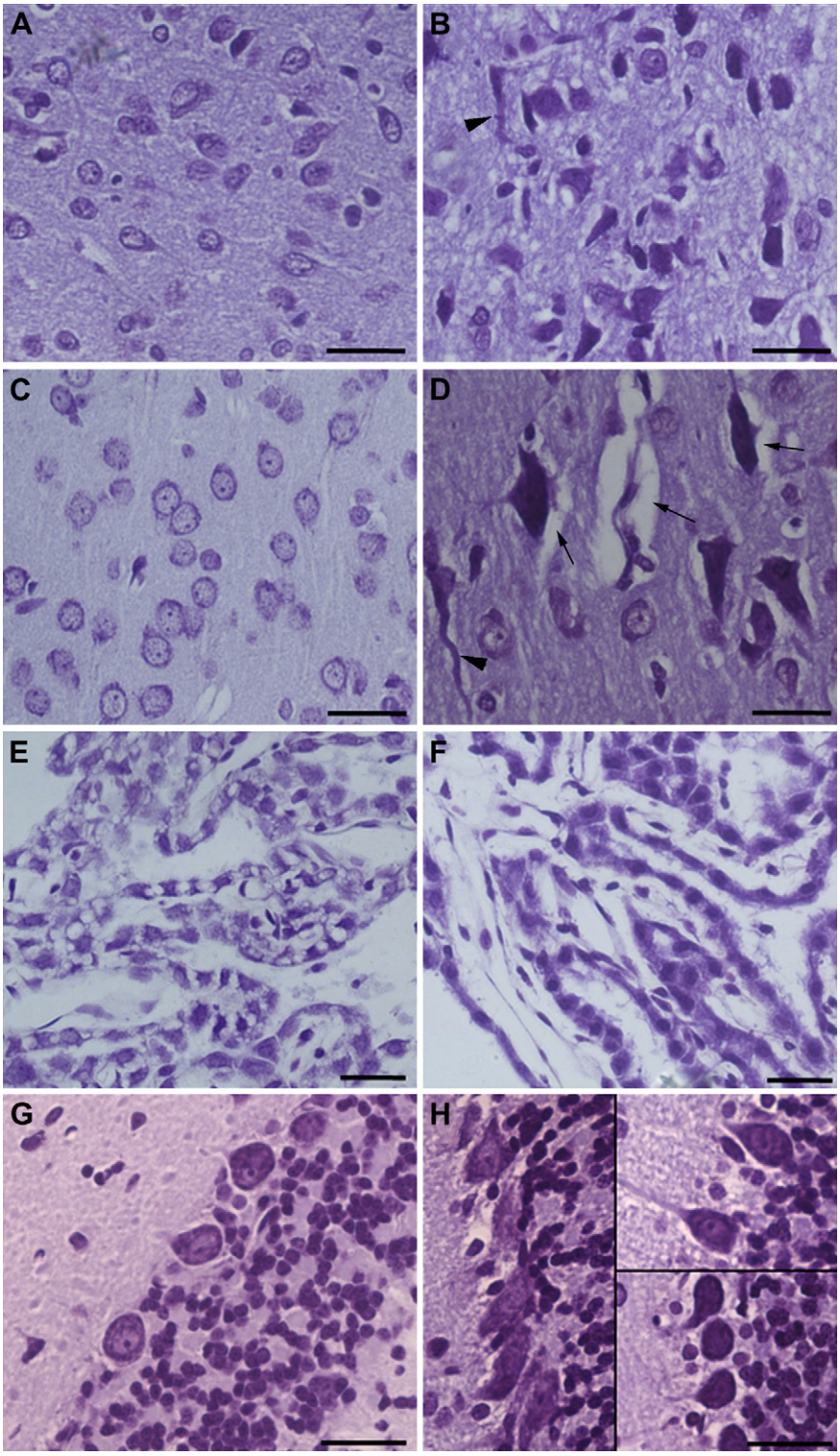

Fig. 1. Pictures of Nissl stained histological sections from rats, 2 days after i.p. injection with *E. Coli* supernatant expressing Stx2 (sStx2) (B, D, F, H), or control supernatant (sCtrl) (A, C, E, G). A and B: periventricular region of the brain; C and D: cerebral cortex; E and F: choroid plexus of lateral ventricle; G and H: cerebellum. Neurons with pyknotic and amorphous nuclei, and hypertrophied axons (arrowheads) were found in brain periventricular regions (B) and cortex (D), and in cerebellar Purkinje cells (H) of sStx2 injected rats. Edema surrounding the cell bodies and vessels (arrows, D), and the loss of epithelial-endothelial organization in the choroid plexus (F), are also shown. Cerebrum and cerebellum of control rats remained preserved (A, C, E, and G). Bars in A–F: 30 μm, and in G, H: 20 μm.

between blood and brain, whereas, AQP4 and AQP1 expressions in the membranes of ependymal cells lining the ventricles indicate AQPs involvement in water movement between brain and cerebrospinal fluid compartments. Alterations of CNS AQPs trigger important changes in brain water balance, being implicated in the development of brain edema. It has been reported that AQP4 deletion aggravates vasogenic brain edema produced by a fluid leak, reducing the rate of water outflow from the brain [30]. In our

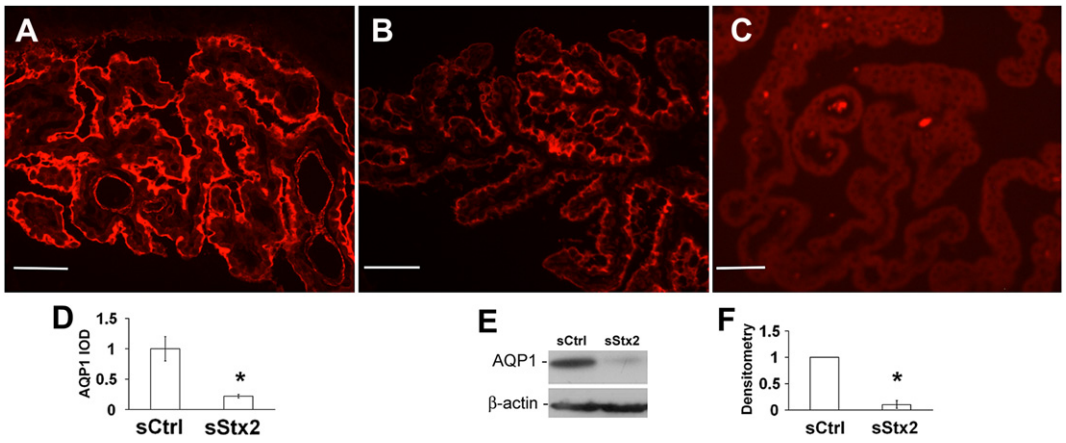

Fig. 2. Microphotographs show the immunofluorescence for AQP1 in choroid plexus of rats, 2 days after i.p. injection with sCtrl (A), or sStx2 (B). Photo in C corresponds to negative control for AQP1 immunofluorescence, with pre-immune serum instead of the primary antibodies. A significant decrease in AQP1 (B) staining is shown in choroid plexus of sStx2 injected rat compared to control (A). Results in D, represent the mean IOD ± SEM of six animals, analyzed with Image J-NIH software; $^{*}p < 0.05$, sStx2 *vs* sCtrl. Densitometric analysis of western blot (E), normalized for β-actin, confirmed the results of AQP1 immunofluorescence. Bars: 100 μm.

studies, the significant decrease of brain AQP4 in sStx2 treated animals may be related to the edema found around neurons of the cerebral cortex and periventricular regions, and in some perivascular areas. The presence of brain edema was previously found in several HUS animal models [18–20]. In addition, it has been demonstrated that Stx is able to increase the brain blood barrier permeability [33]. Edema formation around vessels may occur as a result of the increase in brain blood barrier permeability, allowing the passage of fluid to the extra cellular space, and the decrease in AQPs expression that prevents fluid elimination.

AQP4 is also implicated in clearance of K^{+} released during neuronal activity. The increase in seizure threshold and duration

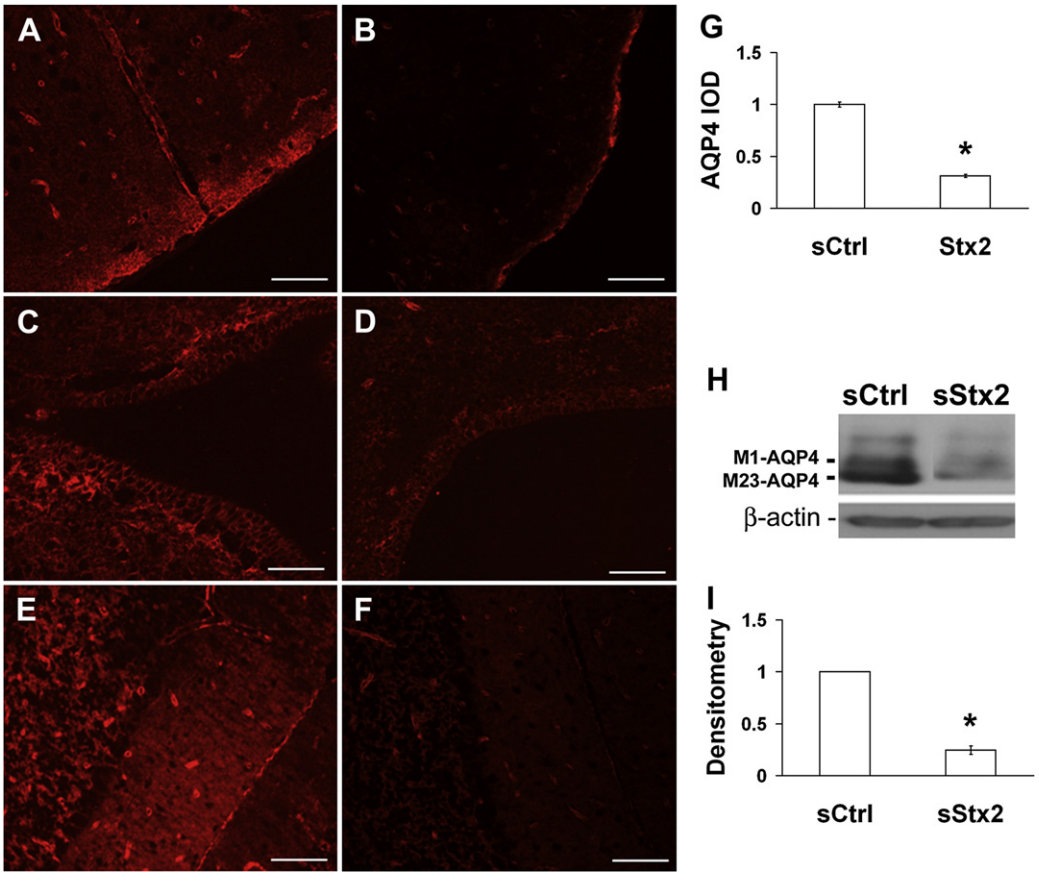

Fig. 3. Microphotographs show the immunofluorescence for AQP4 in subarachnoid space (A and B), epithelium of the ependymal cells surrounding the ventricles (C and D), and cerebellum (E and F). A significant inhibition in the immunostaining of AQP4 was observed in the cerebrum (B and D) and cerebellum (F) of rats, 2 days after sStx2 inoculation, compared to the respective controls (A, C, and E). Results in G, represent the mean IOD ± SEM of six animals, analyzed with Image J-NIH software, $^{*}p < 0.05$, sStx2 *vs* sCtrl. Western blot analysis (H), normalized to beta-actin, showed a decrease of both AQP4-M1 and AQP4-M23 isoforms in total brain samples of sStx2 injected rats, compared to controls. Densitometric analysis of both AQP4 isoforms together is shown in I. Bars: 100 μm.

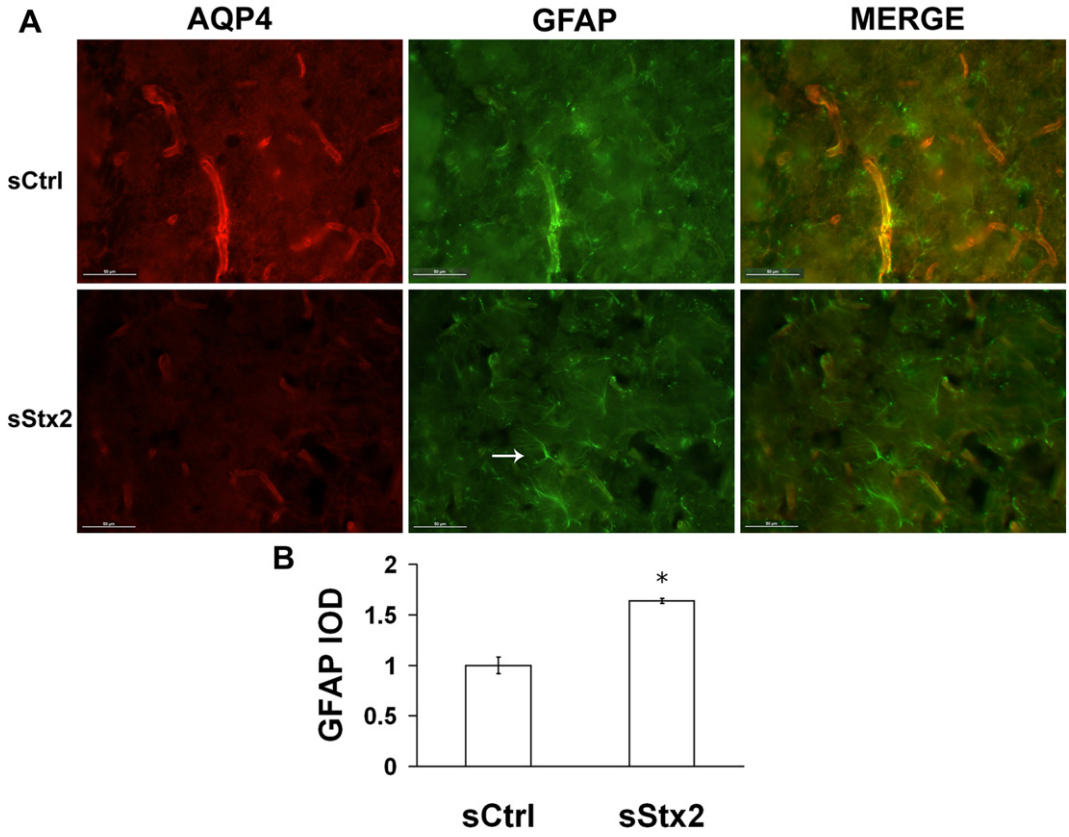

Fig. 4. Double immunofluorescent staining for AQP4 (red) and GFAP (green) showed colocalization in both sCtrl and sStx2 injected rats, in which yellow staining was observed in the astrocytes endfeet surrounding the vessels (A). A higher immunoreactivity for GFAP and lower staining for AQP4 was found in the astrocytes body of rats i.p. injected with sStx2 compared to controls. Pictures show astrocytes in the periventricular region close to lateral ventricles. Results in B, represent the mean IOD ± SEM of three animals, analyzed with Image J-NIH software; $^{*}p < 0.05$, sStx2 *vs* sCtrl. Bars: 50 μm. (For interpretation of the references to color in this figure legend, the reader is referred to the web version of this article.)

was demonstrated in AQP4-null mice [34,35]. The AQP4 down-regulation detected in astrocytes of rats inoculated with sStx2, could reduce the K^{+} clearance from neurons to adjacent astrocytes, resulting in alteration of neuron functionality. Although, edema around neuron bodies was observed, seizures were not evidenced in this group of rats.

Furthermore, the decreased expression of AQP4 in the ependimal epithelium and AQP1 in the epithelium of choroid plexus, found in sStx2 injected rats, may alter cerebrospinal fluid formation. It was reported that AQP1 deletion reduced intracranial pressure and improved survival rate after focal brain injury [36]. However, more studies are necessary to elucidate the implication of SNC water channels alteration in water balance and neurological manifestations during HUS.

In the kidney, both AQP1 and AQP4 are involved in water reabsorption across renal tubular epithelia contributing to urine concentration. AQP1-null mice showed polyuria and defects in the reabsorption of fluid in the proximal tubule [37]. However, deletion of AQP4 in mice showed a very mild urinary concentrating defect [38]. Rats intravenously injected with a non-lethal dose of Stx2, were reported to show an elevation in urinary AQP1 and AQP2 levels, and a reduction in AQP2 protein in the renal plasma membranes of collecting duct principal cells, during polyuric phase of renal failure [39]. However, in our studies rats were inoculated with a letal dose of Stx2, which produced an acute renal failure [31]. These animals became oligoanuric and did not suffer the polyuric phase of the disease.

The significant decrease in AQP1 and AQP4 protein levels observed in brain, could be a consequence of a direct cytotoxic effect of Stx2 on the inhibition of protein synthesis. It is known that Stx2 causes inhibition of protein synthesis and apoptosis in different cell types of the kidney and the CNS [40–43]. However, we have also found an increase in GFAP reactivity in periventricular astrocytes of sStx2 injected animals. Stx is able to stimulate significant cytokines release from astrocytes and other cell types [44,45]. Smith et al. [44], demonstrated that Stx1 induced a ribotoxic stress response in the intestinal epithelial cell line HCT-8, and activated p38 and JNK mitogen-activated protein kinases, resulting in the stimulation of both chemokine expression and apoptosis. Recently, Petruzziello-Pellegrini et al. [46], reported that low concentrations of Stx, which produced approximately 10% inhibition of global protein synthesis, inactivate host ribosomes but can also modulate gene expression and activate selected cell signaling pathways, as CXCR4/CXCR7/SDF-1, that change ribosome function and phenotype of human microvascular endothelial cells. In our studies, the ribotoxic stress produce by Stx2 could affect the expression of brain AQPs, but also selectively stimulate the expression of some genes, resulting in GFAP activation.

Downregulation of brain AQPs could be due also to functional mechanisms. In the brain, vasopressin activates V1 receptors and PKC resulting in the inhibition of AQP4 water permeability [47]. Moreover, dopamine has also been shown to inhibit AQP4 water permeability [47] as well as downregulate AQP4 expression in astrocytes [48]. Nevertheless, it has been reported that dopamine stimulated GFAP expression in astrocytes by activation of p38 MAPK intracellular pathway [49]. As far as we know, there is no information regarding whether dopamine could be implicated during HUS development.

In the present work, AQP4 co-localized with GFAP in astrocytes endfeet of both sCtrl and sStx2 injected rats. The rise on GFAP reactivity, found in the brain of rats i.p. inoculated with sStx2, is consistent with other works in which a direct cytotoxic effect of the toxin was evaluated [17,45,50]. Astrocytes are involved in inflammatory processes, being activated in response to brain injury. Under this event, they may release inflammatory mediators through which may alter the integrity and permeability of the blood brain barrier and the neuronal survival [51]. Moreover, astrocytes may release neurotrophic factors [52] which could be neurotoxic to neurons pursuing brain damage. The inoculation of Stx2 by intracerebroventricular administration also increased GFAP immunofluorescence, evidencing astrogliosis in astrocytes in contact with Stx2-containing neurons [50]. In these studies, astrogliosis was correlated with changes in the expression and activity of neuronal nitric oxide synthase [50]. Active participation of cytokines or neurotrophic factors in our experimental rat model is highly probable. In addition, downregulation of AQP4 in astrocytes may impair K^+ reuptake by astrocytes leading to alteration in neural signal transduction.

Stx and bacterial LPS has been shown to stimulate production of pro-inflammatory cytokines by several cell types, including brain microvascular endothelial cells and astrocytes [45,53,54]. It was reported that Stx1 induced an early inflammatory response in lipopolysaccharide (LPS)-sensitized astrocytes, whereas astrocytes activation and cell death was induced later [45]. LPS, tumor necrosis factor-alpha (TNF-α), and interleukin-1beta (IL-1β) potentiate the cytotoxic effects of Stx by stimulating the expression of Gb3 receptor in the plasma membrane of target cells [41,53,54]. However, it has not been determined yet whether the inflammatory response observed in animal models and patients with HUS could be implicated in the alteration of brain AQPs. IL-1β was shown to induce the expression of AQP4 mRNA and protein through NF-κβ pathway without involvement of *de novo* protein synthesis in rat astrocytes [55]. Contrary to this, another report showed that neither TNF-α nor IL-1β modified AQP1 and AQP4 expression in human astrocytes [56]. On the other hand, the possibility that LPS could be implicated in AQPs modulation in sStx2 injected rats can be excluded, because both sStx and sCtrl supernatants injected to the animals contained equally low ($<$0.03 μg/ml) concentration of LPS. Further studies are in progress to elucidate the mechanisms by which Stx2 altered AQPs expression in rat CNS.

Experimental models of HUS have been developed in different animal species in which renal damage together with CNS disorders were found, same as may happen in children with HUS [15,19,57]. It was demonstrated that Stx is able to cross the blood brain barrier and enter into the CNS, where it was immunodetected in astrocytes and neurons [15,17,58]. In the present study, we have used an experimental model of HUS in rats, in which we had previously demonstrated the development of acute renal failure [31]. Moreover, all rats died 3–5 days after sStx2 inoculation, probably as a result of both renal and extra-renal susceptibility to Stx2.

In conclusion, in the present work we showed neuronal alterations and downregulation of AQP1 and AQP4 in the brain of rats, 2 days after i.p. injection with sStx2. These alterations may be involved in the edema formation and in neurological manifestations characteristic of HUS.

Acknowledgment

This work was supported by grants to C. Silberstein from the Universidad de Buenos Aires (UBACyT M440, and UBACyT 637).

References

[1] Repetto HA. Epidemic hemolytic-uremic syndrome in children. Kidney Int 1997;52:1708–19.
[2] Repetto HA. Long-term course and mechanisms of progression of renal disease in hemolytic uremic syndrome. Kidney Int 2005;(Suppl. 97):S102–6.
[3] Eriksson KJ, Boyd SG, Tasker RC. Acute neurology and neurophysiology of haemolytic-uraemic syndrome. Arch Dis Child 2001;84(5):434–5.
[4] Exeni R. Síndrome Urémico Hemolítico. Arch Latin Nefr Ped 2001;1:35–56.
[5] Oakes RS, Siegler RL, McReynolds MA, Pysher T, Pavia AT. Predictors of fatality in postdiarrheal hemolytic uremic syndrome. Pediatrics 2006;117(5): 1656–62.
[6] Gallo EG, Gianantonio CA. Extrarenal involvement in diarrhoea-associated haemolytic-uraemic syndrome. Pediatr Nephrol 1995;9(1):117–9.
[7] Siegler RL. Spectrum of extrarenal involvement in postdiarrheal hemolytic-uremic syndrome. J Pediatr 1994;125(4):511–8.
[8] Valles PG, Pesle S, Piovano L, Davila E, Peralta M, Principi I, et al. Postdiarrheal Shiga toxin-mediated hemolytic uremic syndrome similar to septic shock. Medicina 2005;65:395–401.
[9] Rivas M, Miliwebsky E, Chinen I, Deza N, Leotta G. The epidemiology of hemolytic uremic syndrome in Argentina. Diagnosis of the etiologic agent, reservoirs and routes of transmission. Medicina 2006;66:27–32.
[10] O'Brien AD, Holmes RK. Shiga and Shiga-like toxins. Microbiol Rev 1987;51: 206–20.
[11] Lingwood CA. Role of verotoxin receptors in pathogenesis. Trends Microbiol 1996;4:147–53.
[12] Sandvig K, Garred O, Prydz K, Kozlov JV, Hansen SH, van Deurs B. Retrograde transport of endocytosed Shiga toxin to the endoplasmic reticulum. Nature 1992;358:510–2.
[13] Endo Y, Tsurugi K, Yutsudo T, Takeda Y, Ogasawara K, Igarashi K. Site of action of a Vero toxin (VT2) from *E coli* O157:H7 and of Shiga toxin on eukaryotic ribosomes. RNA N-glycosidase activity of the toxins. Eur J Biochem 1988;171: 335–7.
[14] Johannes L, Romer W. Shiga toxins-from cell biology to biomedical applications. Nat Rev Microbiol 2010;8(2):105–16.
[15] Obata F, Tohyama K, Bonev AD, Kolling GL, Keepers TR, Gross LK, et al. Shiga toxin 2 affects the central nervous system through receptor globotriaosylceramide localized to neurons. J Infect Dis 2008;198:1398–406.
[16] Tironi-Farinati C, Loidl CF, Boccoli J, Parma Y, Fernandez-Miyakawa ME, Goldstein J. Intracerebroventricular Shiga toxin 2 increases the expression of its receptor globotriaosylceramide and causes dendritic abnormalities. J Neuroimmunol 2010;222:48–61.
[17] Goldstein J, Loid CF, Pistone Creydt V, Boccoli J, Ibarra C. Intracerebroventricular administration of Shiga toxin type 2 induces striatal neuronal death and glia alterations: an ultrastructural study. Brain Res 2007; 1161:106–15.
[18] Tzipori S, Chow CH, Powell HR. Cerebral infection with Escherichia coli 01 57:H7 in humans and gnotobiotic piglets. J Clin Pathol 1988;41:1099–103.
[19] Francis DH, Moxley RA, Andraos CY. Edema disease-like brain lesions in gnotobiotic piglets infected with *Escherichia coli* Serotype 0157:H7. Infect Immun 1989;57(4):1339–42.
[20] Isogai E, Isogai H, Kimura K, Hayashi S, Kubota T, Fujii N, et al. Role of tumor necrosis factor alpha in gnotobiotic mice infected with an *Escherichia coli* O157 :H7 strain. Infect Immun 1998;66:197–202.
[21] Lehmann GL, Gradilone SA, Marinelli RA. Aquaporin water channels in central nervous system. Curr Neurovasc Res 2004;1:293–303.
[22] Yool AJ. Aquaporins: multiple roles in the central nervous system. Neuroscientist 2007;13:470–85.
[23] Zelenina M. Regulation of brain aquaporins. Neurochem Int 2010;57:468–88.
[24] Praetorius J, Nielsen S. Distribution of sodium transporters and aquaporin-1 in the human choroid plexus. Am J Physiol Cell Physiol 2006;291:C59–67.
[25] Nielsen S, Nagelhus EA, Amiry-Moghaddam M, Bourque C, Agre P, Ottersen OP. Specialized membrane domains for water transport in glial cells: high-resolution immunogold cytochemistry of aquaporin-4 in rat brain. J Neurosci 1997;17(1):171–80.
[26] Lu M, Lee MD, Smith BL, Jung JS, Agre P, Verdijk MA, et al. The human AQP4 gene: definition of the locus encoding two water channel polypeptides in brain. Proc Natl Acad Sci U S A 1996;93(20):10908–12.
[27] Furman CS, Gorelick-Feldman DA, Davidson KG, Yasumura T, Neely JD, Agre P, et al. Aquaporin-4 square array assembly: opposing actions of M1 and M23 isoforms. Proc Natl Acad Sci U S A 2003;100(23):13609–14.
[28] Silberstein C, Bouley R, Huang Y, Fang P, Pastor-Soler N, Brown D, et al. Membrane organization and function of M1 and M23 isoforms of aquaporin-4 in epithelial cells. Am J Physiol Renal Physiol 2004;287(3):F501–11.
[29] Amiry-Moghaddam M, Williamson A, Palomba M, Eid T, de Lanerolle NC, Nagelhus EA, et al. Delayed K+ clearance associated with aquaporin-4 mislocalization: phenotypic defects in brains of a-syntrophin-null mice. Proc Natl Acad Sci U S A 2003;100:13615–20.
[30] Verkman AS, Binder DK, Bloch O, Auguste K, Papadopoulos MC. Three distinct roles of aquaporin-4 in brain function revealed by knockout mice. Biochim Biophys Acta 2006;1758(8):1085–93.
[31] Silberstein C, Lucero MS, Zotta E, Copeland DP, Lingyun L, Repetto HA, et al. Glucosylceramide synthase inhibitor protects rats against the cytotoxic effects of Shiga toxin-2. Pediatr Res 2011;69(5):390–4.

[32] Hall WC. Upper motor neuron control of the brainstem and spinal cord. In: Purves D, Augustine GJ, Fitzpatrick D, Hall WC, Lamantia AS, McNamara JO, et al., editors. Neuroscience. 3rd ed. Sunderland (MA):: Sinauer Associates Inc; 2004. p. 393–415.
[33] Fukuda M, Kitaichi K, Abe F, Fujimoto Y, Takagi K, Morishima T, et al. Altered brain penetration of diclofenac and mefenamic acid, but not acetaminophen, in Shiga-like toxin II-treated mice. J Pharmacol Sci 2005;97:525–32.
[34] Binder DK, Oshio K, Ma T, Verkman AS, Manley GT. Increased seizure threshold in mice lacking aquaporin-4 water channels. Neuroreport 2004;15:259–62.
[35] Binder DK, Yao X, Verkman AS, Manley GT. Increased seizure duration in mice lacking aquaporin-4 water channels. Acta Neurochir 2006;(Suppl. 96):389–92.
[36] Oshio K, Watanabe H, Song Y, Verkman AS, Manley GT. Reduced cerebrospinal fluid production and intracranial pressure in mice lacking choroid plexus water channel Aquaporin-1. FASEB J 2005;19(1):76–8.
[37] Schnermann J, Chou C-L, Ma T, Traynor T, Knepper MA, Verkman AS. Defective proximal tubular fluid reabsorption in transgenic aquaporin-1 null mice. Proc Natl Acad Sci U S A 1998;95:9660–4.
[38] Ma T, Yang B, Gillespie A, Carlson EJ, Epstein CJ, Verkman AS. Generation and phenotype of a transgenic knock-out mouse lacking the mercurial-insensitive water channel aquaporin-4. J Clin Invest 1997;100:957–62.
[39] Sugatani J, Komiyama N, Mochizuki T, Hoshino M, Miyamoto D, Igarashi T, et al. Urinary concentrating defect in rats given Shiga toxin: elevation in urinary AQP2 level associated with poliuria. Life Sci 2002;71:171–89.
[40] Fujii J, Wood K, Matsuda F, Carneiro-Filho BA, Schlegel KH, Yutsudo T, et al. Shiga toxin 2 causes apoptosis in human brain microvascular endothelial cells via C/EBPhomologous protein. Infect Immun 2008;76:3679–89.
[41] Pistone Creydt V, Silberstein C, Zotta E, Ibarra C. Cytotoxic effect of Shiga toxin-2 holotoxin and its B subunit on human renal tubular epithelial cells. Microbes Infect 2006;8:410–9.
[42] Silberstein C, Pistone Creydt V, Gerhard E, Núñez P, Ibarra C. Inhibition of water absorption in human proximal tubular epithelial cells in response to Shiga toxin-2. Pediatr Nephrol 2008;23:1981–90.
[43] Rutjes NW, Binnington BA, Smith CR, Maloney MD, Lingwood CA. Differential tissue targeting and pathogenesis of verotoxins 1 and 2 in the mouse animal model. Kidney Int 2002;62:832–45.
[44] Smith WE, Kane AV, Campbell ST, Acheson DWK, Cochran BH, Thorpe CM. Shiga toxin 1 triggers a ribotoxic stress response leading to p38 and JNK activation and induction of apoptosis in intestinal epithelial cells. Infect Immun 2003;71:1497–504.
[45] Landoni VI, de Campos-Nebel M, Schierloh P, Calatayud C, Fernandez GC, Ramos MV, et al. Shiga toxin 1-induced inflammatory response in lipopolysaccharide-sensitized astrocytes is mediated by endogenous tumor necrosis factor alpha. Infect Immun 2010;78(3):1193–201.
[46] Petruzzielo-Pellegrini TN, Yuen DA, Page AV, Patel S, Soltyk AM, Matouk CC, et al. The CXCR4/CXCR7/SDF-1 pathway contributes to the pathogeesis of Shiga toxin-associated hemolytic uremic syndrome in humans and mice. J Clin Invest 2012;122:759–75.
[47] Zelenina M, Zelenin S, Bondar AA, Brismar H, Aperia A. Water permeability of aquaporin-4 is decreased by protein kinase C and dopamine. Am J Physiol Renal Physiol 2002;283:F309–18.
[48] Kuppers E, Gleiser C, Brito V, Wachter B, Pauly T, Hirt B, et al. AQP4 expression in striatal primary cultures is regulated by dopamine-implications for proliferation of astrocytes. Eur J Neurosci 2008;28:2173–82.
[49] Luo Y, Kokkonen GC, Hattori A, Chrest FJ, Roth GS. Dopamine stimulates redox-tyrosine kinase signaling and p38 MAPK in activation of astrocytic C6-D2L cells. Brain Res 1999;850:21–38.
[50] Boccoli J, Loidl CF, Lopez-Costa JJ, Creydt VP, Ibarra C, Goldstein J. Intracerebroventricular administration of Shiga toxin type 2 altered the expression levels of neuronal nitric oxide synthase and glial fibrillary acidic protein in rat brains. Brain Res 2008;1230:320–33.
[51] Abbott NJ. Inflammatory mediators and modulation of blood-brain barrier permeability. Cell Mol Neurobiol 2000;20:131–47.
[52] Pehar M, Cassina P, Vargas MR, Castellanos R, Viera L, Beckman JS, et al. Astrocytic production of nerve growth factor in motor neuron apoptosis: implications for amyotrophic lateral sclerosis. J Neurochem 2004;89:464–73.
[53] Ramegowda M, Samuel J, Tesh V. Interaction of shiga toxins with human brain microvascular endothelial cells: cytokines as sensitizing agents. J Infect Dis 1999;180:1205–13.
[54] Eisenhauer PB, Chaturvedi P, Fine RE, Ritchie AJ, Pober JS, Cleary TG, et al. Tumor necrosis factor alpha increases human cerebral endothelial cell Gb3 and sensitivity to Shiga toxin. Infect Immun 2001;69:1889–94.
[55] Ito H, Yamamoto N, Arima H, Hirate H, Morishima T, Umenishi F, et al. Interleukin-1β induces the expression of aquaporin-4 through a nuclear factor-κß pathway in rat astrocytes. J Neurochem 2006;99:107–18.
[56] Satoh J, Tabunoki H, Yamamura T, Arima K, Konno H. Human astrocytes express aquaporin-1 and aquaporin-4 *in vitro* and *in vivo*. Neuropathology 2007;27:245–56.
[57] Fujii J, Kita T, Yoshida S, Takeda T, Kobayashi H, Tanaka N, et al. Direct evidence of neuron impairment by oral infection with verotoxin-producing Escherichia coli O157:H7 in mitomycin-treated mice. Infect Immun 1994;62:3447–53.
[58] Fujii J, Kinoshita Y, Yamada Y, Yutsudo T, Kita T, Takeda T, et al. Neurotoxicity of intrathecal Shiga toxin 2 and protection by intrathecal injection of anti-Shiga toxin 2 antiserum in rabbits. Microb Pathog 1998;25:139–46.